Entanglement, Einstein Podolsky Rosen correlations and Schrödinger cat state generation by quantum-injected optical parametric amplification

Entanglement, Einstein Podolsky Rosen correlations and Schrődinger cat state generation by quantum-injected optical parametric amplification

Francesco De Martini[1] **and Fabio Sciarrino**[1,2]

[1] Dipartimento di Fisica and Consorzio Nazionale Interuniversitario per le Scienze Fisiche della Materia, Universitá 'La Sapienza', Roma 00185, Italy
[2] Centro di Studi e Ricerche 'Enrico Fermi', Via Panisperna 89/A, Compendio del Viminale, Roma 00184, Italy

Abstract
We investigate the multi-photon quantum superposition state generated by the quantum-injected high-gain optical parametric amplification of a single photon. The physical configurations based on the optimal universal and on the phase-covariant quantum cloning have been adopted. The theoretical results are supported by a set of experiments leading to the generation of an average number of clones in excess of 10^3.

PACS numbers: 42.50.Ar, 89.70.+c, 03.65.Bz, 03.67.−a

(Some figures in this article are in colour only in the electronic version)

1. Introduction

In recent years a large number of experiments aimed at the verification of fundamental aspects of quantum mechanics, such as its intrinsic nonlocality implied by the celebrated Einstein Podolsky Rosen (EPR) argument [1], have been realized by adopting photon particles mutually interacting through a nonlinear optical (NLO) process. In particular, sophisticated NLO methods have been extended to investigations and realizations in the domain of the emerging sciences of quantum information (QI) and quantum communication. As a first example, based on the isomorphism existing between any spin-1/2 qubit, the polarization state of a single photon and/or any couple of photon momenta **k**, the reliable and flexible technique of spontaneous parametric down-conversion (SPDC) has been commonly adopted to create bi-partite polarization entangled figure 1(*a*) [2]. More recently the nonlinear SPDC scheme has been upgraded into a NL parametric amplifier acting on a single-photon input carrier of quantum information, i.e. a quantum-bit (*qubit*) state: $|\phi\rangle$. This process, referred to as 'quantum-injected nonlinear (NL) parametric amplification' (QIOPA) [3] turned out to be particularly fruitful to gain insight into several little explored albeit fundamental, modern
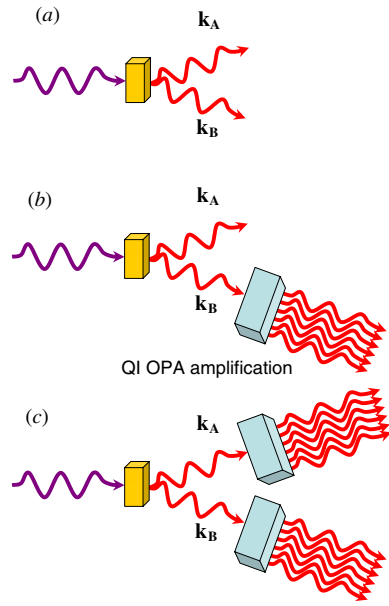
Figure 1. (*a*) Entangled pairs generation by spontaneous parametric down conversion within a nonlinear crystal; (*b*) schematic diagram of the single photon *quantum-injected* optical parametric amplifier (QIOPA); (*c*) optical parametric amplification of both output modes $\mathbf{k}_A$ and $\mathbf{k}_B$.

aspects of QI. For instance it allowed recently the realization of a set of 'optimal' quantum 'cloning' transformations, i.e. able to transform a general input N qubit state, onto a system of higher dimension, $M > N$ by providing at the same time the optimal distribution of the information contained in the original system [2, 4, 5] . Precisely, referring to the QIOPA device that will be described shortly, there it is generally supposed that N photons, identically prepared in an arbitrary state of polarization ($|\phi\rangle$), are injected into the amplifier, or 'cloner' on the input mode $\mathbf{k}_1$. The QIOPA then generates on the same mode $\mathbf{k}_1$, referred to as the 'cloning mode' (C), $M > N$ copies, or *clones* of the input $|\phi\rangle$. Moreover, in the case of the mode-nondegenerate QIOPA, the device simultaneously generates $M - N$ states $|\phi^\perp\rangle$ on the output *anticloning* mode $\mathbf{k}_2$ (AC) thus realizing on that mode a quantum NOT gate.

In the last years, the QIOPA scheme has been at the basis of experimental realizations of the $1 \to 2$ universal optimal quantum cloning machine (UOQCM) [2, 6–9] and of the $1 \to 3$ phase-covariant quantum cloning machine (PCQM) [10] . Recently these tests, carried out originally in low power linearized conditions, i.e. with very low values of the parametric 'gain' parameter $g \ll 1$, were followed by a series of high-gain (HG) spontaneous and stimulated OPA works, where $g > 1$ was raised to the highest values allowed by the damage properties of the NL crystal, leading to the generation of a large number of output particles M. First experiments involving ∼10 photons have been reported recently [11–13], last improvement have led to an output field in excess of 10^3 particles. Within this $N \to M$ cloning endeavour, a multi-photon superposition entangled state was generated, indeed a Schrődinger cat state (SCS) [12, 14, 15]. Precisely, in virtue of the quantum-coherence preserving property of the parametric process, the SCS process implied the deterministic transfer of the well accessible and easily achievable quantum superposition condition affecting any input single-particle qubit to a 'mesoscopic', i.e. multi-particle, amplified quantum-superposition.
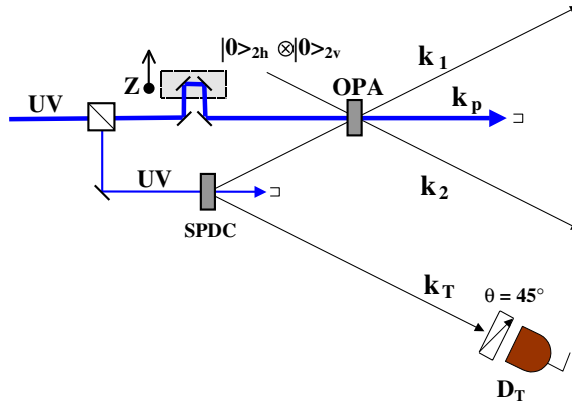
Figure 2. Schematic diagram of the *quantum-injected* optical parametric amplifier (QIOPA) in *entangled configuration*. The injection is provided by an external spontaneous parametric down conversion source of polarization entangled photon states [3].

In the context of quantum nonlocality and of bipartite entanglement, the diagrams reported in figure 1 summarize the conceptual innovation realized by the present work and its possible evolution in the future. While, since 1935 the nonlocal correlations were thought to connect the dynamics of two 'microscopic' objects, i.e. two spins within the well-known EPR-Bohm scheme here represented by diagram (*a*), in diagram (*b*) the entanglement is established, via a single cloning amplification, between a 'microscopic' and a 'macroscopic', i.e. multi-particle, quantum object. At last, the adoption of two independent QIOPA's acting over the two entangled modes would establish bipartite nonlocal correlations between two 'macroscopic' bodies (*c*).

In this paper we describe the quantum analysis of the quantum-injected parametric amplifier in the two different 'mode non-degenerate' and 'mode degenerate' dynamical configurations. Moreover, a description of the experimental apparatus will be given and the most relevant results will be presented. A final discussion undertaken in the conceptual framework of quantum nonlocality will consider the intrinsic limitations of the present method.

The creation of the entangled mesoscopic system is represented by the schematic diagram shown in figure 2 [3]. A nonlinear (NL) crystal, excited by a strong coherent UV laser pulse, is created by spontaneous parametric down-conversion (SPDC) π-entangled EPR photon couples. A single photon belonging to any couple, associated with the mode $\mathbf{k}_T$ and detected by detector D_T is the 'trigger' of the conditional experiment. The twin photon, associated with mode $\mathbf{k}_1$ is injected into another NL crystal, which provides the optical parametric amplification (OPA). By an optical filtering apparatus acting on the trigger photon, it is possible to determine non-locally the quantum state, i.e. the *qubit* of the injected photon. According to previous investigations, the overall QI-OPA apparatus realizes on the output modes $\mathbf{k}_1$ and $\mathbf{k}_2$ respectively the 'optimal cloning' and the 'optimal orthogonalization' of the input qubit [3, 6–8]. A most appealing feature of this high-gain QIOPA cloning system consists of its quantum nonlocal character implied by the entanglement affecting the cloning and anti-cloning output modes in the *multi-particle* condition $\mathbf{k}_1$ and $\mathbf{k}_2$ as well as the trigger mode $\mathbf{k}_T$. Such a scheme has been experimentally implemented adopting 'folded' configurations that adopt a single NL crystal slab excited in both directions to realize in succession the SPDC and the QI-OPA operations. As said, this apparatus was found to realize the deterministic $1 \rightarrow M$ *universal optimal quantum cloning machine* (UOQCM), i.e., able to copy optimally

any unknown input qubit into $M \gg 1$ copies with the same 'fidelity'. The section 2 of this paper is entirely devoted to the description of this apparatus.

In the second 'collinear' configuration, the main result of the present paper, described in details in section 3, two different NL crystals were used and the two output modes $\mathbf{k}_j$ ($j = 1, 2$) were made to collapse into a single mode [16]. This configuration exploits the process of *phase-covariant cloning*. This transformation realizes the optimal distribution of quantum information contained from a single qubit into many ones for qubits restricted to a subspace of the Bloch sphere [10]. Specifically, here we consider the phase-covariant process for equatorial qubits: $|\phi\rangle = 2^{-1/2}(|0\rangle + e^{i\varphi}|1\rangle)$. The partial *a-priori* information on the qubit to be cloned allows us to achieve higher fidelity and, in the present scheme, higher visibility of the coherence of the multi-photon quantum superposition generated. In view of the novelty and intrinsic interest of the phase-covariant cloning process section 3 is devoted to the analysis of this condition. Innovative aspects of the present approach have been achieved both in the experimental setup, which exploits for the first time a collinear configuration in a stimulated emission regime, either in the adopted techniques to characterize the output state. Fringe patterns have been observed for output fields involving up to 1400 photons. A higher visibility has been obtained measuring second-order correlation functions.

2. Quantum injected parametric quantum cloner: non-degenerate case

Let us consider the experimental scheme reported in figure 2. A single photon (mode $\mathbf{k}_1$) is injected into the nonlinear (NL) crystal, typically a BBO (β-barium-borate), cut for type II phase matching and excited by a sequence of UV (ultra-violet) mode-locked laser pulses of wavelength (wl) λ_p propagating along the mode $\mathbf{k}_P$. The relevant modes of the NL three-wave interaction driven by the UV pulses associated with mode $\mathbf{k}_p$ are the two spatial modes with wave-vector (wv) $\mathbf{k}_i$, $i = 1, 2$, each one supporting the two horizontal (H) and vertical (V) polarizations of the interacting photons. The QIOPA is λ-degenerate, i.e. the interacting photons have the same wl's $\lambda = 2\lambda_p$. The injected single photon is provided by an external spontaneous parametric down conversion source of biphoton states [3].

Let us refer to the actual implementation, i.e. to the apparatus shown in figure 3. The active element was a BBO crystal, able to generate $\overrightarrow{\pi}$-entangled photons pairs by spontaneous parametric down conversion. The exciting beam was provided by a Ti:Sa coherent MIRA mode-locked laser further amplified by a Ti-Sa regenerative REGA device (**A**) operating with pulse duration 180 fs at a repetition rate 250 kHz, average power 1 W. The laser frequency doubled by second harmonic generation (SHG) provided the excitation beam of UV wavelength (wl) $\lambda_P = 397.5$ nm and energy per pulse $E_{UV}^{HG} = 1$ μJ. The 'seed' photons pairs were emitted, with a coherence time $\approx$500 fs, by a SPDC process acting towards the right-hand side (rhs) of figure 3 with equal wl's $\lambda = 795$ nm over two spatial modes $-\mathbf{k}_1$ and $-\mathbf{k}_2$ owing to a SPDC process excited by the UV beam associated with mode $-\mathbf{k}_p$ with wl λ_p. The UV beam was back-reflected over the mode $\mathbf{k}_p$ onto the NL crystal by a spherical mirror $\mathbf{M}_p$, with μ-metrically adjustable position **Z**, thus exciting the main OPA 'cloning' process towards the left-hand side of figure 3. By the combined effect of two adjustable optical UV wave-plates (wp's) ($\lambda/2 + \lambda/4$) acting on the projections of the linear polarization π_p^{UV} on the optical axis of the BBO crystal for the $-\mathbf{k}_p$ and $\mathbf{k}_p$ excitation processes, the 'seed' SPDC excitation was always kept at a low level while driving the main OPA to a large gain (HG) regime. Precisely, by smartly unbalancing the orientation of the axes of the UV $wp's$, the SPDC emission probability towards the rhs of figure 3 of two simultaneous photon pairs was always kept below that of single pair emission by a factor $\sim 3 \times 10^{-2}$. One of the photons of the 'seed' SPDC pair, back-reflected by a fixed mirror **M**, was *re-injected* after a $\overrightarrow{\pi}$-flipping
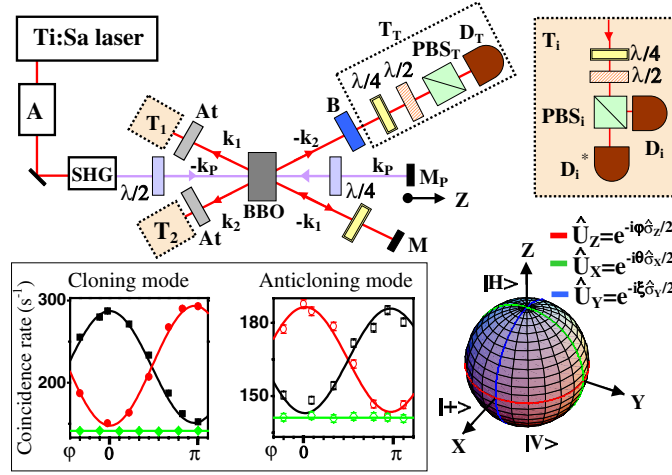
Figure 3. Layout of the *quantum-injected OPA* apparatus; T_i ($i = 1, 2$): analysis and detection apparatus; Bloch sphere representation of the input qubit. Inset: interference fringe patterns measured over the modes $\mathbf{k}_i$ versus the phase φ for the $\widehat{U}_Z$ map. The continuous lines express the best fit results.

by a $\lambda/4$ wp, onto the NL crystal over the input mode $\mathbf{k}_1$, while the other photon emitted over mode ($-\mathbf{k}_2$) excited the detector D_T, the trigger of the overall conditional experiment. The entangled state of the 'seed' pair after M-reflection and $\overrightarrow{\pi}$ -flipping was

$$|\Phi^-\rangle_{-k2,k1} = 2^{-1/2} \left(|H\rangle_{-k2}|H\rangle_{k1} - |V\rangle_{-k2}|V\rangle_{k1} \right). \tag{1}$$

In virtue of the nonlocal correlation acting on the 'seed' modes $-\mathbf{k}_1$ and $-\mathbf{k}_2$, the input qubit was prepared on mode $\mathbf{k}_1$ in the *pure* state $|\Psi\rangle_{\text{in}} = \alpha|H\rangle_{k1} + \beta|V\rangle_{k1}$, $|\alpha|^2 + |\beta|^2 = 1$ by the combined action of the $\lambda/2$ wp, of $\lambda/4$ wp (WP_T), of the adjustable Babinet compensator (B) and of a polarizing beam-splitter (PBS$_T$) acting on mode $-\mathbf{k}_2$. This device allowed all orthogonal transformations $\widehat{U}_X, \widehat{U}_Y, \widehat{U}_Z$ on the Bloch sphere of the input qubit: figure 3, inset. The detection apparatus T_T, T_i ($i = 1, 2$) were equipped with equal single-photon fibre-coupled SPCM-AQR14-FC detectors (D) with quantum efficiencies $\eta_D \simeq 60\%$ and interference filters with bandwidth $\Delta\lambda = 4.5$ nm placed in front of each of them: figure 3, inset.

Let us re-write $|\Psi\rangle_{\text{in}}$ by expressing the interfering states as Fock product states: $|H\rangle_{k1} = |1\rangle_{1H}|0\rangle_{1V}|0\rangle_{2H}|0\rangle_{2V} \equiv |1, 0, 0, 0\rangle$; $|V\rangle_{k1} = |0, 1, 0, 0\rangle$, accounting for one photon on the input $\mathbf{k}_1$ with different orthogonal $\overrightarrow{\pi}'s$ and vacuum on the input $\mathbf{k}_2$. It evolves into the output state $|\Psi\rangle = \widehat{U}|\Psi\rangle_{\text{in}}$ according to the main OPA unitary $\widehat{U}$ process [8]. The output state $\widetilde{\rho} = (|\Psi\rangle\langle\Psi|)$ over the modes $\mathbf{k}_1, \mathbf{k}_2$ of the QI-OPA apparatus is found to be expressed by the expression

$$|\Psi\rangle = \alpha|\Psi\rangle^H + \beta|\Psi\rangle^V, \tag{2}$$

where

$$|\Psi\rangle^H = \sum_{i,j=0}^{\infty} \gamma_{ij}\sqrt{i+1}\,|i+1, j, j, i\rangle \tag{3}$$

$$|\Psi\rangle^V = \sum_{i,j=0}^{\infty} \gamma_{ij}\sqrt{j+1}\,|i, j+1, j, i\rangle, \tag{4}$$

with $\gamma_{ij} \equiv (-\Gamma)^i \Gamma^j \cosh^{-3} g$, $\Gamma \equiv \tanh g$, the parameter g expressing the NL 'gain' [7]. These interfering entangled, multi-particle states are *orthonormal*, i.e. $|^i\langle \Psi \mid \Psi \rangle^j|^2 = \delta_{ij} \{i, j = H, V\}$ and pure, i.e. represented by the operators: $\rho^H = (|\Psi\rangle\langle\Psi|)^H$, $\rho^V = (|\Psi\rangle\langle\Psi|)^V$. Hence the pure state $|\Psi\rangle$ is a quantum superposition of two multi-photon pure states and bears the same superposition properties of the injected qubit. In addition, it is significant in the present context to consider the output pure state $|\Sigma\rangle$ of the overall apparatus, including the 'trigger', which enters into the dynamics through the Bell state $|\Phi^-\rangle_{-k2,k1}$. This state, commonly referred to as a '*Schrödinger cat state*' [14], expresses the entanglement of all output modes $\mathbf{k}_1, \mathbf{k}_2$ and $-\mathbf{k}_2$, thus eliciting a peculiar cause–effect dynamics within the overall 'closed' system

$$|\Sigma\rangle \equiv 2^{-1/2}(|H\rangle_{-k2}|\Psi\rangle^H - |V\rangle_{-k2}|\Psi\rangle^V). \tag{5}$$
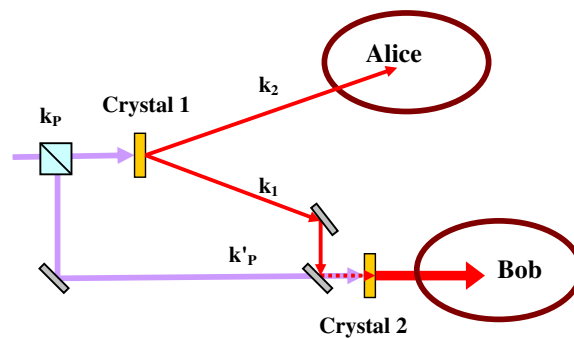
The experimental investigation of the multi-photon superposition and entanglement implied by equations (2) and (5) was carried out by means of the T_i, T_T devices according to a 'loss method' first applied to SPDC by [11]. The beams associated with the output modes $\mathbf{k}_i$ ($i = 1, 2$) were attenuated down to the single-photon level by the two low transmittivity BS's (At) in figure 3. The maximum value of the 'gain' $g_{\exp}$ and of the overall quantum efficiencies η_i of the detection apparatuses acting on $\mathbf{k}_i$ ($i = 1, 2$) were measured. It was found: $g_{\exp} = 1.19 \pm 0.05$ and $\eta_1 = (4.9 \pm 0.2)\%$; $\eta_2 = (4.2 \pm 0.2)\%$.

Let us now address the main goal of the present section, i.e., the detection and characterization of the output states. The interference character of the output field implied by the quantum superposition feature of the input qubit $|\Psi\rangle_{\mathrm{in}} = 2^{-1/2}(|H\rangle + e^{i\varphi}|V\rangle)$ was detected simultaneously in the basis $|\pm\rangle \equiv 2^{-1/2}(|H\rangle \pm |V\rangle)$ over the output 'cloning' mode, $\mathbf{k}_1$ and 'anticloning', $\mathbf{k}_2$ by the $2 - D$ coincidences $[D_i, D_T]$ (square marks in figure 3 inset) and $[D_i^*, D_T]$ (circle marks) ($i = 1, 2$). Precisely, the interference fringe patterns correspond to $\widehat{U}_Z$ transformations on the input Bloch sphere, i.e. implying changes of the phase φ. The fringe 'visibility' ($\mathcal{V}$) measured over $\mathbf{k}_1$ was found to be gain-dependent $\mathcal{V}_1^{\mathrm{th}}(g) = (1 + 2\Gamma^2)^{-1}$ as predicted by theory [3]. The experimental value $\mathcal{V}_1 = (32 \pm 1)\%$ should be compared with the theoretical one: $\mathcal{V}_1^{\mathrm{th}}(g_{\exp}) = 42\%$. By setting $g = \Gamma = 0$ the effective visibility of the input qubit was measured: $\mathcal{V}_{\mathrm{in}} \approx 87\%$. The $\mathcal{V}$-value for the $\mathbf{k}_2$ mode $\mathcal{V}_2 = (13 \pm 1)\%$ should be compared with the theoretical one: $\mathcal{V}_2^{\mathrm{th}} = 33\%$ [3]. All these discrepancies are mainly attributed to unavoidable walk-off effects in the NL slab spoiling the critical superposition of the injection and pump pulses in the bi-refringent active region. The overall average number of the stimulated emission photons per pulse over $\mathbf{k}_i$ ($i = 1, 2$) was found, in the quantum-injected HG regime, $M = (11.1 \pm 1.3)$, a result consistent with the value of g measured by a different experiment. Precisely, the average number of photons generated on the cloning mode was $M_C = 6.1 \pm 0.9$ and the average 'fidelity', obtained by the corresponding $\mathcal{V}$-value on the same mode, was $F_C = (1 + V_1)/2 = 66.2 \pm 0.5$. Note that for $M \to \infty$, viz. $g \to \infty$ and $\Gamma \to 1$, the 'fringe visibility' and the 'fidelity' attain the asymptotic values $\mathcal{V}_1^{\mathrm{th}} = \mathcal{V}_2^{\mathrm{th}} = 33\%$ and $F_C = F_{AC} = (2/3)$. In the present experiment, because of the unavailability on the market of reliable photon number-resolving detectors, the measurement of M and M_C was transformed into a detection rate measurement owing to $\eta_1 \sim \eta_2 \ll 1$.

3. Multi-particle superposition by phase-covariant cloning

Let us now describe the configuration based on a phase-covariant cloning process on the basis of figure 4. The 'rationale' of the experiment can be briefly outlined as follows [16]. An entangled polarization state of two photons was generated by a NL crystal 1 pumped by an ultraviolet (UV) pump beam propagating over the mode $\mathbf{k}_P$.

Figure 4. Optical configuration of the phase-covariant quantum-injected optical parametric amplifier. The SPDC quantum injector (crystal 1) is provided by a type II generator of polarization entangled photon couples. Crystal 2, realizing the OPA action, is cut for collinear type II phase matching.

Precisely, the entangled photon pair emitted over the modes $\mathbf{k}_1$ and $\mathbf{k}_2$ was found to be in the quantum state

$$|\Psi^-\rangle_{k1,k2} = \frac{1}{\sqrt{2}}\left(|H\rangle_{k1}|V\rangle_{k2} - |V\rangle_{k1}|H\rangle_{k2}\right). \tag{6}$$

While the photon associated with mode $\mathbf{k}_2$ is coupled into a single mode fibre (referred to as trigger mode) and freely propagates, the single photon state generated over the mode $\mathbf{k}_1$ is injected, together with an UV pump beam (mode $\mathbf{k}'_P$), into the nonlinear crystal 2 and stimulates the emission of many photon pairs. The multi-particle amplified quantum-state keeps the same quantum superposition character of the input in virtue of the information-preserving (i.e. coherence-preserving) property of the optical parametric amplification. After the amplification process, the output quantum state reads

$$\frac{1}{\sqrt{2}}\left(|\Phi\rangle_{k1}^H|V\rangle_{k2} - |\Phi\rangle_{k1}^V|H\rangle_{k2}\right), \tag{7}$$

where the wavefunctions $|\Phi\rangle^H$ and $|\Phi\rangle^V$ now involve 10^2–10^3 photons depending on the UV pump power, the efficiency of the nonlinear process, and the adopted geometrical configuration. In summary, the two partners Alice and Bob share an entangled state between a single photon field and a many particles one.

Let us now consider the overall process in deeper detail. The input state is

$$|\Phi_{\text{in}}\rangle = \frac{|H\rangle_{k1} + e^{i\varphi}|V\rangle_{k1}}{\sqrt{2}}. \tag{8}$$

Let us re-write $|\Phi\rangle_{\text{in}}$ by expressing the interfering states as Fock product states: $|H\rangle_{k1} = |1\rangle_{1H}|0\rangle_{1V}$ and $|V\rangle_{k1} = |0\rangle_{1H}|1\rangle_{1V}$. The interaction Hamiltonian of the optical parametric amplification (crystal 2) $\widehat{H}_{\text{coll}} = i\chi\hbar\left(\widehat{a}_H^\dagger\widehat{a}_V^\dagger\right) + \text{h.c.}$ acts on the single spatial mode $\mathbf{k}_1$. The OPA process induces a unitary transformation on the couple of time-dependent field operators: $\widehat{a}_H^\dagger(t)$ and $\widehat{a}_V^\dagger(t)$ for which, at the initial time of the NL interaction, $t = 0$, is $\left[\widehat{a}_i, \widehat{a}_i^\dagger\right] = 1$ and $\left[\widehat{a}_H, \widehat{a}_V^\dagger\right] = 0$. A quantum analysis of the dynamics leads to a linear dependence of the field operators on the corresponding input quantities:

$$\begin{bmatrix} \widehat{a}_H(t) \\ \widehat{a}_V^\dagger(t) \end{bmatrix} = \begin{bmatrix} C & S \\ S & C \end{bmatrix} \begin{bmatrix} \widehat{a}_H(0) \\ \widehat{a}_V^\dagger(0) \end{bmatrix}, \tag{9}$$

where $C = \cosh g$, $S = \sinh g$, $g = \chi t =$ amplification gain, χ is the coupling term proportional to the product of the second-order NL susceptibility of the crystal and of the pump field, assumed classical and undepleted by the interaction. The evolution operator is then expressed in the form of the squeeze operator: $\widehat{U}_A(t) = \exp[g(\widehat{A^+} - \widehat{A})]$, where $\widehat{A^+} = \widehat{a}_V^\dagger(t)\widehat{a}_H^\dagger(t)$ and $\widehat{A} = \widehat{a}_V(t)\widehat{a}_H(t)$. The injected state evolves into the output state $|\Phi\rangle = \widehat{U}_A |\Phi_{\mathrm{in}}\rangle$. By use of the disentangling theorem, the output state is found to be

$$|\Phi\rangle = |\Phi\rangle^H + \mathrm{e}^{\mathrm{i}\varphi}|\Phi\rangle^V, \tag{10}$$

with

$$|\Phi\rangle^H = \frac{4}{C^2} \sum_{n=0}^{\infty} \Gamma^n \sqrt{n+1} \, |n+1\rangle_{1H} \, |n\rangle_{1V} \tag{11}$$

$$|\Phi\rangle^V = \frac{4}{C^2} \sum_{n=0}^{\infty} \Gamma^n \sqrt{n+1} \, |n\rangle_{1H} |n+1\rangle_{1V}, \tag{12}$$

where $\Gamma = S/C$.

Hence the pure state $|\Phi\rangle$ is a quantum superposition of two multi-photon *pure states* and bears the *same* superposition properties of the injected qubit. In addition in the present context, it is significant to consider the output *pure* state of the *overall* apparatus, including the 'trigger' that enters in the dynamics through the Bell state $|\Psi^-\rangle_{k1,k2}$:

$$|\Pi\rangle \equiv 2^{-1/2}(|H\rangle_{k2}|\Phi\rangle^V - |V\rangle_{k2}|\Phi\rangle^H). \tag{13}$$

The *entanglement entropy* $\mathcal{E}(|\Pi\rangle)$ of $\widetilde{\rho}' \equiv |\Pi\rangle\langle\Pi|$ is expressed by the Von Neumann entropy of either the k_2 or OPA subsystem: $\mathcal{E}(|\Pi\rangle) = S(\widetilde{\rho}_{k2}) = S(\widetilde{\rho}_{k1}) = 1$, being $\widetilde{\rho}_{k2} = \mathrm{Tr}_{k1}(\widetilde{\rho}')$, $\widetilde{\rho}_{k1} = \mathrm{Tr}_{k2}(\widetilde{\rho}')$ and $S(\widetilde{\rho}_j) = -\mathrm{Tr}(\widetilde{\rho}_j \log_2 \widetilde{\rho}_j)$ [8]. The maximal attainable value is $\mathcal{E}(|\Pi\rangle) = 1$ for the output bipartite system.

3.1. Experimental setup

The excitation source was a Ti:Sa coherent MIRA mode-locked laser further amplified by a Ti:Sa regenerative REGA device operating with pulse duration 180 fs at a repetition rate of 250 kHz. Improvements in the amplifier cavity have led to an overall output power equal to 1.5 W. The output beam, frequency-doubled by second harmonic generation (SHG), provided the excitation beam of UV wavelength (wl) $\lambda_P = 397.5$ nm and power 650 mW. Consider the diagram shown in figure 5: two BBO (β-barium borate) NL crystals cut for type II phase matching, were excited by two beams derived from the common UV laser at wavelength λ_P through a $\lambda/2$ wp and a polarizing beam splitter. By appropriate orientation of the wp acting on linear polarized UV, the seed SPDC excitation was always kept at a low level while driving the main OPA to a high-gain (HG) regime. Crystal 1, excited by the UV beam $\mathbf{k}_P'$, was the SPDC source of π-entangled photon couples of wl $\lambda = 2\lambda_P$, emitted over the two output modes $\mathbf{k}_i$ ($i = 1, 2$). The pump power of beam $\mathbf{k}_P'$ was set in order to have a negligible probability to generate two pairs of photons. The photon emitted over $\mathbf{k}_1$ provided the quantum injection into the OPA, physically consisting of the NL crystal 2 cut and oriented for collinear operation over the two linear polarization modes, respectively parallel and orthogonal to the horizontal.

One of the photons of the 'seed' SPDC pair was injected, after undergoing a $\overrightarrow{\pi}$-rotation by a $\lambda/2$ wp, into the second NL crystal over the input mode $\mathbf{k}_1$, while the other photon emitted over mode $\mathbf{k}_2$ excited the detector D_T, the trigger of the overall conditional experiment. The entangled state of the 'seed' pair was $|\Psi^-\rangle_{k1,k2} = 2^{-1/2}(|H\rangle_{k1}|V\rangle_{k2} - |V\rangle_{k1}|H\rangle_{k2})$. In virtue
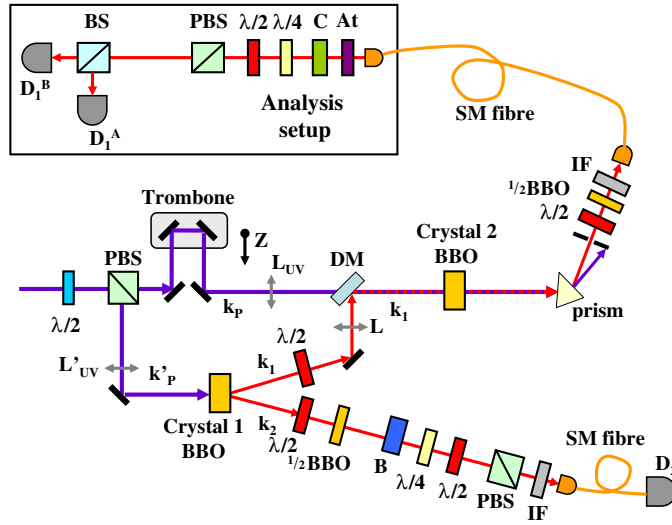
Figure 5. Experimental setup.

of the nonlocal correlation acting on the 'seed' modes $\mathbf{k}_1$ and $\mathbf{k}_2$, the input qubit was prepared on mode $\mathbf{k}_1$ in the *pure* state $|\Psi\rangle_{\text{in}} = \alpha|H\rangle_{k1} + \beta|V\rangle_{k1}$, $|\alpha|^2 + |\beta|^2 = 1$ by the combined action of the $\lambda/2$ wp, of $\lambda/4$ wp (WP_T), of the adjustable *Babinet compensator* (B) and of a polarizing beam-splitter (PBS$_T$) acting on mode $-\mathbf{k}_2$. By a 'trombone' device with micrometrically adjustable position Z, the time superposition in the OPA of the excitation UV pulse and of the injection photon wavepacket was ensured. The injected single photon and the UV pump beam $\mathbf{k}_P$ were superposed exploiting a dichroic mirror (DM) with high reflectivity at λ and high transmittivity at λ_P.

The output state of the crystal 2 with wl λ was spatially separated by the fundamental UV beam through prism dispersion, then spectrally filtered adopting an interferential filter (IF) with bandwidth equal to 1.5 nm and then coupled to a single mode fibre. A $\lambda/2$ waveplate and a BBO with thickness of 0.75 mm provided the compensation of walk-off effects. At the output of the fibre, after compensation (C) of the polarization rotation induced by the fibre, the radiation field was attenuated (At), analysed combining waveplates ($\lambda/2 + \lambda/4$ wp) and polarizing beam splitter (PBS) and detected adopting single photon detectors SPCM-AQR14 (D_1^A and D_1^B).

3.1.1. Estimation of the gain value. In a first experiment without quantum injection, we estimated the gain value g of the optical parametric process and the overall quantum efficiency of the detection apparatus. The count rates of D_1^A were measured for different values of the UV power (figure 6). The plots of figure 6(*a*) clearly show the onset of the NL parametric interaction for large values of g, thus implying the generation of many photon pairs. The gain value of the process is obtained by fitting the count rates N_1 of detector D_1^A, depending on the UV pump power P_{UV}, with the function $N_1(g) = R\frac{\eta_1\Gamma^2}{1-(1-\eta_1)\Gamma^2}$ [11], where $\Gamma = \tanh g$, η_1 is the quantum efficiency of the overall detection process on mode $\mathbf{k}_1$ and R is the repetition rate of the pump source. The gain value g depends on the UV power, namely $g = \gamma\sqrt{P_{UV}}$, where the parameter γ takes into account the efficiency of the NL process. The maximal gain value obtained has been found $g_{\text{max}} = (3.05 \pm 0.03)$, which leads to a mean photon number

(a)

(b)
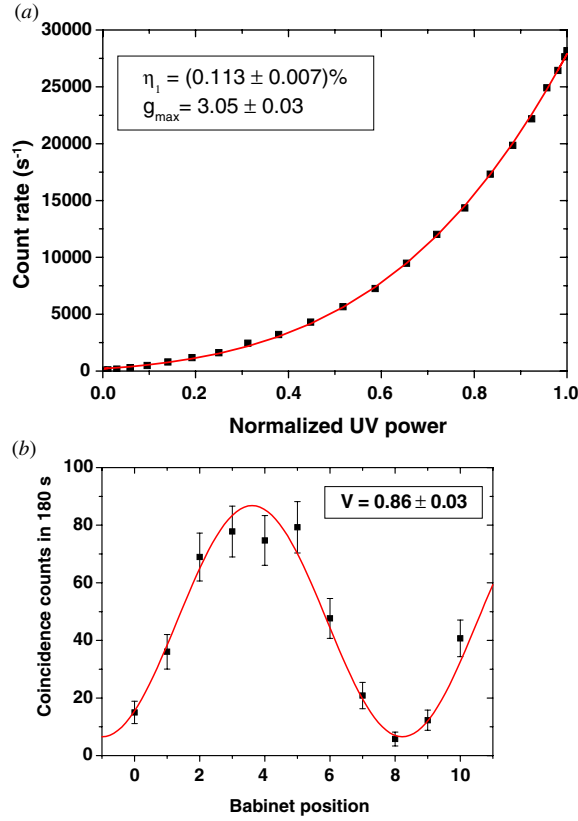
Figure 6. (a) Count rates of $[D_1^A]$ as a function of the normalized UV power. The continuous line expresses the best fit result. (b) Coherence detection between trigger and cloning in the basis $|\pm\rangle \equiv 2^{-1/2}(|H\rangle \pm |V\rangle)$: coincidences versus phase angle φ when the amplifier is turned off $(g = 0)$.

per mode $\bar{n} = \sinh^2 g_{\max} = (111 \pm 7)$. In conclusion the maximal total number of generated photon on $\mathbf{k}_1$ mode through the SPDC process is $M = 2\bar{n} = (222 \pm 14)$. By means of the previous fit, we could also estimate the overall detection efficiency η_1 on the $\mathbf{k}_1$ mode, which results form the glass attenuation (At), the fibre coupling, and the quantum detection efficiency of the detector: $\eta_1 = (1.13 \pm 0.07) \times 10^{-3}$. By the previous values we find $\eta\bar{n} \simeq 0.1$.

3.1.2. Quantum coherence. The interference character of the output field implied by the quantum superposition character of the input qubit $|\Psi\rangle_{\rm in} = 2^{-1/2}(|H\rangle + {\rm e}^{i\varphi}|V\rangle)$ was detected in the basis $|\pm\rangle \equiv 2^{-1/2}(|H\rangle \pm |V\rangle)$ over the output 'cloning' mode, $\mathbf{k}_1$ by the $2 - D$ coincidences $\left[D_1^A, D_T\right]$. The fringe 'visibility' ($\mathcal{V}$) measured over $\mathbf{k}_1$ was found to be gain-dependent $\mathcal{V}^{\rm th-1}(g) = \frac{2\bar{n}+1}{4\bar{n}+1}$ as predicted by theory [16]. By setting $g = \Gamma = 0$ the effective visibility of the input qubit was measured: $\mathcal{V}_{\rm in} = (86 \pm 3)\%$ (figure 6(b)). The last value differs from the unit value mainly for the emission of double pairs from the crystal; indeed by subtracting estimated accidental coincidences the visibility is found to be $(95 \pm 3)\%$ (figure 7(a)). By turning on the optical amplifier, we observed the experimental value $\mathcal{V}^{\rm exp-1} = (17.8 \pm 0.6)\%$ which should be compared with the theoretical one: $\mathcal{V}^{\rm th-1}(g_{\rm exp}) = 50.1\%$.
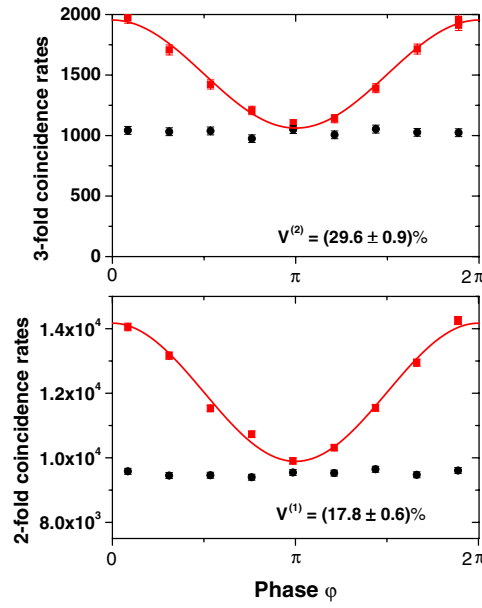
Figure 7. Square dots: coincidences between trigger and cloning mode versus phase delay φ ($g = 3.05$). Circle dots: coincidences between trigger and cloning mode without quantum injection.

The second-order fringe 'visibility' ($\mathcal{V}$) measured over $\mathbf{k}_1$ through triple coincidences of the detectors $\left[D_1^A, D_1^B, D_T \right]$ was found to be gain-dependent $\mathcal{V}^{th-2}(g) = \frac{12\bar{n}^2 + 8\bar{n}}{18\bar{n}^2 + 10\bar{n}}$ as predicted by theory [16]. The experimental value $\mathcal{V}^{exp-2} = (29.6 \pm 0.9)\%$ should be compared with the theoretical one: $\mathcal{V}^{th-2}(g_{exp}) = 66.7\%$ (figure 7(b)). Partial mismatches between amplifying pump beam and input single photon state are the main causes of the discrepancy between expected and experimental visibilities (figure 7).

In the quantum-injected HG regime, the overall average number of the stimulated emission photons *per pulse* over $\mathbf{k}_1$ was found, $M = (289 \pm 18)$, a result consistent with the value of g measured by an entirely different experiment. The average 'fidelity', obtained by the corresponding V-value on the same mode, was $F_C = (1 + \mathcal{V}^{th-1})/2 = 0.589 \pm 0.003$. Note that for $M \to \infty$, viz. $g \to \infty$ and $\Gamma \to 1$, the 'fringe visibility' and the 'fidelity' attain the asymptotic values $\mathcal{V}^{th-1} = 50\%$, $F_C = 3/4$, and $\mathcal{V}^{th-2} = 66.66\%$. These values correspond the fidelity of optimal phase estimation. There, analogously to the optimal universal cloning, a tight relation between the quantum cloning process and the theory of quantum measurement is found. In the present experiment, in absence of reliable photon number-resolving detectors, the measurement of M and M_C was transformed into a detection rate measurement as $\eta_1 \ll 1$.

Improvements in the geometry of the pumping beam have led to an increase of the gain parameter $g_{max} = (3.89 \pm 0.04)$, corresponding to a mean photon number in the stimulated regime 1434 ± 30. In the last condition an experimental visibility equal to $\mathcal{V}^{exp-1} = (15.1 \pm 0.9)\%$ has been observed.

4. Conclusions

An interesting property of the present system is its resilience to de-coherence as shown by the interference patterns of figures 3 and 7. Since in our system de-coherence is only determined by

stray reflection losses on the single output surface of the NL crystal, a photon number $M \simeq 10^3$ could be easily excited in quantum superposition. This result is partially attributed to the minimum Hilbert–Schmidt (d) 'distance' on the phase-space of the interfering states realized here: $d(\rho^H; \rho^V) = \text{Tr}[(\rho^H - \rho^V)^2] = 2$ [17]. The limited, but *optimal,* distinguishability of the mesoscopic states is attributed to the present single particle, *cloningwise,* π-measurement method. However, the *exact* distinguishability implied by the orthogonality of $|\Psi\rangle^H$ and $|\Psi\rangle^V$ could be attained by any POVM identifying in a *cumulative* fashion all M output particles. While in the asymptotic limit $M \to \infty$ single clone fidelity is practically equal to the optimal state estimation or phase estimation depending on the cloning device (either universal or phase-covariant), the amount of information contained by a subset of the output clones deserves further investigation.

In summary, we have demonstrated the interference of mesoscopic, orthonormal, pure states in agreement with the quantum theoretical results, equations (2) and (8). On a conceptual side our system is expected to open a trend of studies on the persistence of the validity of crucial laws of quantum mechanics for entangled mixed-state systems of increasing complexity, on the realization of GHZ processes and on the violation of Bell inequalities in the multi-particles regime [18].

Acknowledgments

References

[1] Einstein A, Podolsky B and Rosen N 1935 *Phys. Rev.* **47** 777
[2] De Martini F and Sciarrino F 2005 *Prog. Quantum Electron.* **29** 165
[3] De Martini F 1998 *Phys. Rev. Lett.* **81** 2842
[4] Scarani V, Iblisdir S, Gisin N and Acín A 2005 *Rev. Mod. Phys.* **77** 1225
[5] Cerf N J and Fiurasek J 2005 *Preprint* quant-ph/0512172
[6] Lamas-Linares A, Simon C, Howell J C and Bouwmeester D 2002 *Science* **296** 712
[7] De Martini F, Bužek V, Sciarrino F and Sias C 2002 *Nature* **419** 815
[8] Pelliccia D, Schettini V, Sciarrino F, Sias C and De Martini F 2003 *Phys. Rev.* A **68** 042306
[9] De Martini F, Pelliccia D and Sciarrino F 2004 *Phys. Rev. Lett.* **92** 067901
[10] Sciarrino F and De Martini F 2005 *Phys. Rev.* A **72** 062313
[11] Eisenberg H S, Khoury G, Durkin G A, Simon C and Bouwmeester D 2004 *Phys. Rev. Lett.* **93** 193901
[12] De Martini F, Sciarrino F and Secondi V 2005 *Phys. Rev. Lett.* **95** 240401
[13] Caminati M, De Martini F, Perris R, Sciarrino F and Secondi V 2006 *Phys. Rev.* A **73** 032312
[14] Schleich W P 2001 *Quantum Opt. Phase Space* (New York: Wiley) chapters 11 and 16
[15] Schroedinger E 1935 *Naturwissenshaften* **23** 807
[16] De Martini F 1998 *Phys. Lett.* A **250** 15
[17] Nielsen M A and Chuang I L 2000 *Quantum Computation and Quantum Information* (Cambridge: Cambridge University Press)
[18] Reid M D *et al* 2002 *Phys. Rev.* A **66** 033801